Quantum Electronics **35** (9) 769 – 777 (2005)

INVITED PAPER

PACS numbers: 52.57.Bc
DOI: 10.1070/QE2005v035n09ABEH006128

Use of conic targets in inertial confinement fusion

I.K. Krasyuk, A.Yu. Semenov, A.A. Charakhch'yan

***Abstract*. Conic targets are shown to be a promising object for the investigation of cumulative effects, which allow the achievement of high energy densities, and their use in experiments involving highly concentrated energy fluxes can open up new possibilities for investigating the physical properties of matter at extremely high temperatures, pressures, and densities. We outline the main experimental and theoretical results obtained to date that are related to conic target investigations and discuss their several possible applications in the future.**

Keywords: *conic targets, thermonuclear reactions, cumulative effects.*

1. Introduction

The progress in the development and construction of high-power pulsed energy sources enables investigating the properties of matter at extremely high temperatures and pressures. To realise these conditions, high-power energy fluxes are directed to targets of different degrees of complexity – ranging from planar to multilayer spherical targets. Among these targets, a special place is occupied by conic targets, which were first proposed [1] for generating high-temperature plasmas to realise controlled thermonuclear fusion.

A conic target is a conic cavity in a high-density solid material filled with gaseous deuterium or its mixture with tritium (Fig. 1a). The gas is retained by a plane or convex thin-walled shell. During the interaction with a concentrated energy flux of a high-velocity piston, the target shell moves into the target with a high velocity to compress and heat the gas contained in it.

The interest in conic targets is caused by several reasons. First, being a part of a spherical volume, conic targets filled with a thermonuclear fuel can be a convenient model of shell spherical targets, which have found wide use in experiments on inertial thermonuclear fusion. In this case, the processes occurring in spherical targets could be possibly simulated by using conic targets at energy fluxes $\Omega/4\pi$ times lower than for spherical targets (where Ω is the solid angle occupied by the conic target). Second, by using a conic target, it is possible to initiate the fusion reaction in a small volume and then use the liberated energy to ignite the bulk of the fuel. Finally, conic targets are candidates for realising cumulative effects in order to attain high energy densities.

I.K. Krasyuk, A.Yu. Semenov A.M. Prokhorov General Physics Institute, Russian Academy of Sciences, ul. Vavilova 38, 119991 Moscow, Russia; e-mail: krasyuk@kapella.gpi.ru, semenov99@rambler.ru;
A.A. Charakhch'yan A.A. Dorodnitsyn Computing Centre, Russian Academy of Sciences, ul. Vavilova 40, 119991 Moscow, Russia; e-mail: chara@ccas.ru

Received 6 June 2005
Kvantovaya Elektronika **35** (9) 769 – 777 (2005)
Translated by E.N. Ragozin

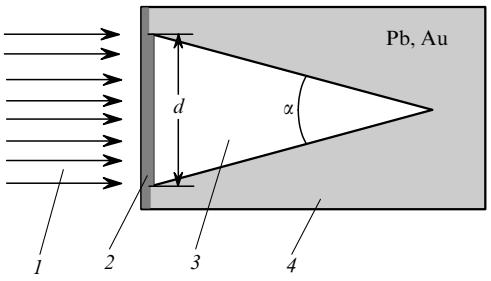

a

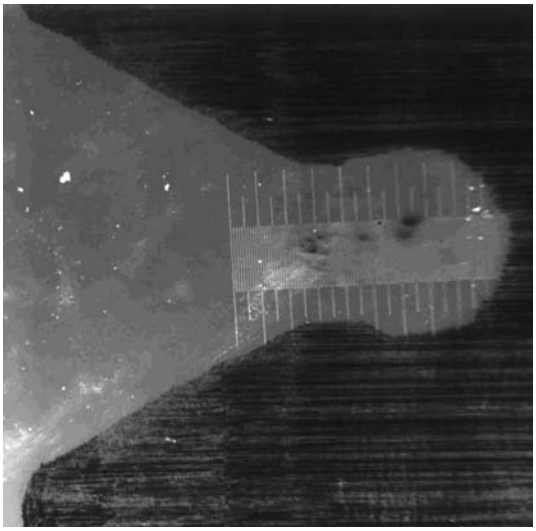

b

Figure 1. Scheme of a conic target (a) and its microsection after laser irradiation under the experimental conditions [7, 8] (the large microscope-scale division is 0.1 mm) (b): (*1*) concentrated energy beam; (*2*) plane or spherical target shell; (*3*) gaseous deuterium or a deuterium–tritium mixture; (*4*) plastic material of the high-density target (lead or gold).

This review outlines the main experimental and theoretical results pertaining to the investigation of conic targets obtained to the present time. The emphasis was placed on the works performed with participation of the authors of this paper.

2. Brief review of experimental results

We begin with a brief chronological review of the main experimental data obtained by different authors in the investigation of conic targets. Then, we outline in greater detail the results of similar experimental investigations carried out at the A.M. Prokhorov General Physics Institute, the Russian Academy of Sciences.

To accelerate the target shell in experiments with conic targets, different techniques were used: the beam (relativistic electron-beam), laser, and explosion techniques. In all instances, a neutron yield was recorded when the conic target was filled with gaseous deuterium or a deuterium–tritium mixture, which testifies to the realisation of nuclear fusion reactions in these experiments.

In Ref [2], experiments were performed with targets in the form of a conic cavity in lead ($\alpha = 60^\circ$, $d = 2$ mm) filled with gaseous deuterium at a pressure of 0.2 atm with the addition of 7 % Ar. The 10-μm thick polyethylene target shell was accelerated to a velocity of 50–70 km s^{-1} by using the energy of an X-ray radiation pulse generated by irradiating (for 30 ns) an additional external target shell (gold or platinum 5 μm in thickness) by a relativistic 1.5-kJ electron beam. The highest recorded neutron yield amounted to $(1-3)\times 10^6$ neutrons per pulse. Theoretical estimates suggested that the deuterium plasma was compressed by a factor of 1000 and heated to a temperature of 1 keV.

In Ref. [3], a target was made in the form of a conic cavity in gold ($\alpha = 60^\circ$, $d = 2$ mm) filled with gaseous deuterium at a pressure of 1.2 atm. The 100-μm thick polyethylene target shell was accelerated to a velocity of 50 km s^{-1} employing a chemical explosive in a special device which employed the cumulative effect. The yield recorded in these experiments was 3×10^7 neutrons per pulse. The authors' estimates showed that the thermonuclear fusion in this case takes place in 1000-fold compressed deuterium at a temperature of about 0.51 keV. Theoretical estimates of the results expected were presented in Ref. [4] and a detailed review of these experiments was given in Refs [5, 6].

In Refs [7, 8], experiments were performed with targets in the form of a conic cavity in lead ($\alpha = 53^\circ$ and 30°, $d = 2$ mm) filled with gaseous deuterium at a pressure of 0.2–1 atm. The 1–5 μm thick target shells of polyethylene terephthalate ($[C_{10}O_4H_8]_n$ with a density of 1.38 g cm^{-3}) were accelerated upon irradiation by 22-ns, 70-J pulses from a neodymium laser. In these experiments, the maximum target shell velocity achieved 150 km s^{-1} and the highest-recorded neutron yield was 4×10^4 neutrons per pulse.

In Ref. [9], a target was made in the form of a conic cavity in lead ($\alpha = 40^\circ$, $d = 0.138$ mm) filled with a gaseous deuterium–tritium mixture at a pressure of 2 atm. The 13-μm thick target shell of polyvinyl alcohol was accelerated by 1.2-ns, 160-J pulses from a CO_2 laser. The neutron yield amounted to 2.8×10^5 neutrons per laser shot.

In Ref. [10], experiments were performed with conic targets with the same parameters as in Ref. [7] ($\alpha = 53^\circ$, $d = 2$ mm). The plane aluminium target shell with a thickness of 0.25–0.3 mm was accelerated to a velocity of 5.4 km s^{-1} with the help of a linear explosive launching system based on an explosive material. A neutron yield of 10^6 neutrons per pulse was recorded in these experiments. The explosive launching system was subsequently improved. To increase the velocity of a 30-μm thick aluminium target shell up to 18 km s^{-1}, use was made of a layered launching system with a 100-μm thick molybdenum plunger accelerated to a velocity of 10 km s^{-1}. This allowed a several-fold increase in the neutron yield. An estimate of deuterium plasma parameters at the final (as regards the neutron yield) stage of the process yielded the following values: a pressure of 60 Mbar, a 3400-fold degree of compression, and the peak temperature of 240 eV.

In Refs [11, 12], experiments were performed with targets in the form of a conic cavity in stainless steel ($\alpha = 60^\circ$, $d = 3.2$ mm) filled with gaseous deuterium at a pressure up to 6 atm. The 130-μm thick target shell of stainless steel was accelerated due to the cumulation of a converging hemispherical shock wave in a gaseous hydrogen–oxygen mixture. The neutron yield was $\sim 10^3$ neutrons per pulse.

In Ref. [13], experiments were conducted with targets in the form of a conic cavity in lead ($\alpha = 60^\circ$, $d = 0.3-0.8$ mm) filled with gaseous deuterium (or a deuterium–tritium mixture) at a pressure of 0.1–1 atm. The 10-μm thick polyethylene target shell was accelerated due to the expansion of an aluminium foil exploding under the action of a 2-μs, 25-kV voltage pulse. When the target was filled with the deuterium–tritium mixture, it was possible to record a neutron yield above the detection threshold (the numerical value of the threshold was not indicated in the paper). In Ref. [13] the first brief review of the experiments with conic targets was presented.

The main data obtained in the experimental investigations with conic targets are presented in Table 1.

3. Main experimental results obtained upon laser irradiation of conic targets and discussion

The experimental study of quantitative characteristics of processes occurring inside conic targets is complicated by the absence of reliable direct techniques of their diagnostics. Among the presently available papers, the greatest quantity of experimental data about the physical processes in conic targets was obtained in the works involving laser irradiation of conic targets [14]. They are fully presented in proceeding [15]. Table 2 gives the data about the initial characteristics of the targets used, the experimental conditions and the results of these experiments.

The experiments were performed on a neodymium-glass laser setup. The laser emitted 1.06-μm, 22-ns, 70-J pulses. The target shell velocities v were measured by recording (with a streak camera) the Doppler frequency shift of the laser radiation backscattered from the target (Fig. 2). With a high accuracy, their temporal dependences can be approximated by the expression

$$v(t) = \left(\frac{\dot{m}u}{a}\right)^{1/2}\frac{1-B_0}{1+B_0},\quad B_0 = \left(1-\frac{t}{t_v}\right)^q,\quad q = 2\left(\frac{au}{\dot{m}}\right)^{1/2},$$

$$\dot{m} = \frac{m_0}{t_v}. \qquad (1)$$

Table 1. Results of experiments on thermonuclear plasma generation in conic targets.

Energy source	Target exposure parameters			Target							N	Year	References
	E/J	t_p/ns	v/km s^{-1}	Wall material	d/mm	α/deg	Shell material	h/μm	Gas	p_0/atm			
REB	1.5×10^3	30	50–70	lead	2	60	polyethylene	10	D_2 + 7 % Ar	0.2	$(1-3) \times 10^6$	1976	[2]
CEM	–	–	50	gold	2	60	polyethylene	100	D_2	1.2	3×10^7	1977	[3]
Nd laser	70	22	to 150	lead	2	53 30	polyethylene terephthalate	1 3 5	D_2	0.2–1	4×10^4	1977 1978	[7] [8]
CO_2 laser	160	1.2	40	lead	0.132	40	polyvinyl alcohol	13	DT	2	2.8×10^5	1979	[9]
CEM	–	–	5.4 18	lead	2	53 30	aluminium foil	250 30	D_2	0.7	$(1-4) \times 10^6$	1980	[10]
CEM	–	–	–	stainless steel	3.2	60	stainless steel	130	D_2	up to 6	$\sim 10^3$	1982	[11, 12]
Electrical foil explosion	20×10^3	2×10^3	5–10	lead	0.3–0.8	60	polyethylene	10–25	D_2 DT	0.2–1	above detection threshold	1984	[13]

Notes: REB – relativistic electron beam; CEM – chemical explosive material; E – radiation energy; t_p – pulse duration; v – target shell velocity; d – input diameter of the conic cavity; α – target cone angle; h – shell thickness; p_0 – gas pressure; N – neutron yield.

Table 2. Target parameters, experimental conditions, and results of experiments obtained upon the laser irradiation of conic targets.

Experiment number	α/deg	h/μm	p_D/atm	r_0/mm	m_D/10^{-7} g	E_0/J	N/10^4	u/10^6 cm s^{-1}	T/keV	t/ns	m_0/t_v/10^4 g cm^{-2} s^{-1}	p_a/10^6 atm	v_{max}/10^6 cm s^{-1}	x/mm
1	30	3	1.0	2.6	7.1	46	3.1	1.33	2.9	35.2	1.2	15.7	9.4	0.42
2	30	3	0.5	3.4	3.6	48	2.8	1.33	6.1	44.5	0.9	12.4	11.8	0.56
3	30	3	0.5	3.4	3.6	54	3.2	1.06	6.9	32.1	1.3	13.7	12.4	0.34
4	30	3	0.2	5.3	1.4	57	3.3	1.06	18.1	42.2	1.0	10.4	17.1	0.45
5	30	1	0.5	1.9	3.6	55	4.0	2.37	7.0	18.7	0.8	18.1	14.3	0.47
6	30	1	0.2	3.0	1.4	53	2.2	0.55	16.8	9.7	1.4	7.8	14.8	0.05
7	30	3	0.5	3.4	3.6	52	2.5	0.35	6.6	19.4	2.1	7.5	9.2	0.07
8	30	3	0.5	3.4	3.6	46	1.0	0.89	5.8	22.9	1.8	16.1	13.5	0.20
9	30	1	1.0	1.3	7.1	53	2.2	2.32	3.4	18.7	0.7	17.1	9.8	0.35
10	30	1	0.8	1.5	5.7	58	3.2	0.28	4.6	10.1	1.4	3.7	9.6	0.03
11	53	3	0.2	2.7	2.6	57	1.4	1.59	39.0	26.0	1.6	25.3	13.3	0.38
12	53	3	0.5	3.4	1.7	55	1.5	1.56	15.1	23.3	1.8	27.8	17.7	0.36
13	53	1	0.5	1.9	1.7	54	2.2	1.40	14.8	6.8	2.0	28.4	17.9	0.10
14	53	5	0.5	4.5	1.7	41	1.4	0.74	11.2	31.9	2.2	16.0	13.4	0.24
15	53	5	1.0	3.4	3.3	46	2.2	1.64	6.3	33.6	2.1	33.7	13.8	0.50
16	53	3	0.5	3.4	1.7	46	2.0	0.73	12.6	24.8	1.7	12.2	11.7	0.18
17	53	5	0.5	4.5	1.7	61	2.3	1.10	16.7	28.8	2.4	26.3	17.2	0.32
18	53	1	1.0	1.3	3.3	52	1.7	1.33	7.1	16.4	0.8	11.2	7.9	0.19

Notes: α – target cone angle; h – shell thickness; p_D and m_D – pressure and mass of deuterium in the target; r_0 – radius of shell curvature; E – energy of laser radiation pulse; N – neutron yield; u – vapour flow velocity; T – calculated average deuterium temperature; t_v – total shell evaporation time; m_0 – initial shell mass per unit area; p_a – average ablative pressure acting on the shell; v_{max} – maximum shell velocity; x – distance traversed by the shell during the laser pulse.

which was derived employing the jet propulsion model of a variable-mass body taking into account its drag in the deuterium atmosphere. The parameter $a = (\gamma+1)\rho/2$ (where γ is the adiabatic exponent of the gas and ρ is its density) in expression (1) characterises the decelerating properties of the atmosphere; u is the vapour flow velocity relative to the moving body; m_0 is the mass of a unit shell area; and t_v is the time required for total evaporation of the shell upon laser irradiation. For $t \to t_v$, the shell velocity approaches its maximum value $v_{max} = (\dot{m}u/a)^{1/2}$. The values of u, t_v, and v_{max} are given in Table 2 for every experiment. Passage to the limit for $a \to 0$ (the absence of drag) transforms expression (1) to

$$v(t) = -u \ln\left(1 - \frac{t}{t_v}\right) = u \ln \frac{m_0}{m(t)}. \quad (2)$$

It was experimentally found that about 15 % of the total energy of a laser pulse incident onto the target finds its way into the target interior. This energy consists of the kinetic energy of the non-evaporated part of the shell (1 %) and the sum of the thermal and kinetic energies (14 %) of the laser plume attached to it. Figure 1b shows the microsection of one of the targets after laser irradiation. One can see that the microexplosion at the target apex gives rise to a spherical cavity, which is symmetric with respect to the cone axis. The target wall is displaced under the action of the pressure pulse

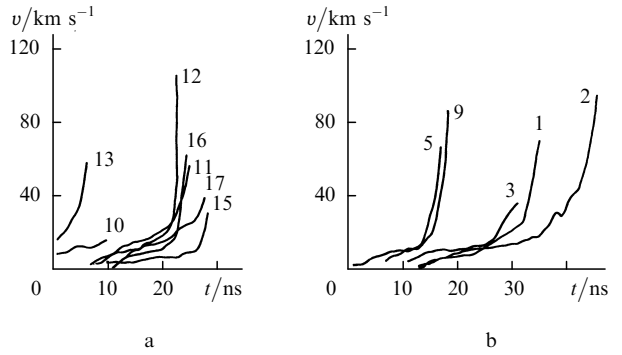

Figure 2. Experimentally measured $v-t$ diagrams of the motion of target shells with the cone angles $\alpha = 30^\circ$ (a) and 53° (b) [15]. The curve numbers correspond to the experiment numbers in Table 2.

and high plasma temperature produced during laser ablation of the target shell and the compression and heating of the gas filling the target. The mass of the plasma cloud flying into the target can be approximately estimated by putting $v(t) = u$ in (2). It is equal to m_0/e, where e is the base of natural logarithm.

Measurements of the electron temperature T_e of the plasma plume by a two-foil absorption technique using 20- and 100-μm thick beryllium filters yielded a value of 40 eV. By using the method of polyethylene terephthalate target shell deceleration in the air or xenon atmosphere, the rate of mass evaporation from a unit area $\dot{m}$ (in units of g cm^{-2} s^{-1}) was determined as a function of the laser radiation intensity I in the $(0.1-1)\times 10^{11}$ W cm^{-2} range [16]:

$$\dot{m} = (1.6 \pm 0.1) \times 10^4 \left[I/(10^{11}\ \mathrm{W\ cm^{-2}})\right]^{1.6\pm0.1}. \qquad (3)$$

The electrocontact probe technique was used to measure the electric field distribution in the plasma corona attached to the target shell. The electric field intensity in the plasma corona amounted to $\sim$1 kV cm^{-1}.

To estimate the parameters of the deuterium plasma produced at the final stage of its compression and heating at the centre of the conic target, the data from the experiments presented in Table 2 (see, for instance, Refs [14, 15, 17, 18]) were subjected to statistical processing. We illustrate the statistical approach as applied to the D–D fusion reaction. It is well known that the total number N of neutrons per pulse arising from the D–D thermonuclear fusion reaction for a uniformly heated deuterium plasma is calculated by the expression

$$N = 0.65 \times 10^{-14} n^2 V\tau (kT)^{-2/3} \exp\left[-18.76(kT)^{-1/3}\right],$$

where n and V are the density (in cm^{-3}) and volume (in cm^3) of the deuterium plasma uniformly heated to a temperature kT (in keV) and τ is the duration of the fusion reaction (in seconds). Let us assume that $\tau = \delta r/c_s$, where r is the radius of the plasma region, c_s is the sound velocity, and δ is the proportionality coefficient. We also introduce an additional proportionality coefficient μ equal to the ratio between the mass m of deuterium heated to the temperature kT and the total mass of target-filling deuterium m_D, i.e. $\mu = m/m_D$. Under these assumption, $n^2 \sim (m_D/r^3)^2$, $V \sim r^3$, $\tau \sim r/c_s \sim rT^{-1/2}$, and then the functional factor $n^2 V\tau T^{-2/3}$ in front of the exponential term in the expression for the neutron yield takes the form

$$n^2 V\tau T^{-2/3} \sim \left(\frac{m_D}{r^3}\right)^2 r^3 r T^{-1/2} T^{-2/3} = \left(\frac{m_D}{r^3} r\right) m_D T^{-7/6}$$

$$= \langle \rho r \rangle m_D T^{-7/6}.$$

Taking into account all proportionality coefficients, the values of physical constants, and the dimensions of the quantities, we eventually obtain a relationship for N in the form

$$N = 2.53 \times 10^{25} \langle \rho r \rangle m_D \mu\delta (kT)^{-7/6} \exp[-18.76(kT)^{-1/3}].$$

After taking the logarithm of this expression, it can be represented in the form of linear relationship $Y = AX + B$, where it is assumed that the variables X and Y contain only experimentally measured quantities and that the coefficients A and B are made up of required unknown quantities, in this case μ and δ. In particular, when the quantities N, $\langle \rho r \rangle$, and kT are known from experiments, then

$$X = 18.76(kT)^{-1/3}, \quad Y = -\ln \frac{N(kT)^{7/6}}{2.53 \times 10^{25} \langle \rho r \rangle m_D},$$

$$A = -\ln(\mu\delta),\ B = 1.$$

If the values of X and Y group together about some straight line in a series of experiments, this will indicate to a regular and similar character of the processes occurring in the thermonuclear targets from experiment to experiment, which permits estimating, in particular, the magnitude of $\mu\delta$, because $A \approx$ const.

Consider now another case when the measurements of, for example, temperature are lacking. By making several additional assumptions, it is possible to obtain the expression for the temperature, provided that the new measurable parameters X and Y group together along a straight line again. In particular, an examination of the experimental data on the interaction of laser radiation with conic targets showed that in this case the assumption is justified that $kT = \beta\varepsilon/m_D$, where m_D is the mass of deuterium which fills the target (in units of 10^{-3} g), ε is the absorbed laser radiation (in Joules), and β is the proportionality factor. Then, we used the measurable quantities

$$X = 18.76(\varepsilon/m_D)^{-1/3},$$

$$Y = -\ln \frac{NV_0(\Omega/4\pi)^{4/3}(\varepsilon/m_D)^{7/6}}{2.53 \times 10^{25} m_D^2 (3V_0/4\pi)^{1/3}},$$

as new variables, where Ω is the solid angle of the conic target and V_0 is its volume (in cm^3). In these variables X and Y, experimental points grouped together along a straight line with the correlation coefficient $R = 0.99$ (Fig. 3). In this case,

$$A = -\ln\left(\mu^{4/3}\delta\xi^{2/3}\beta^{-7/6}\right) = 9.77 \pm 0.41,$$

$$B = \beta^{-1/3} = 2.82 \pm 0.12,$$

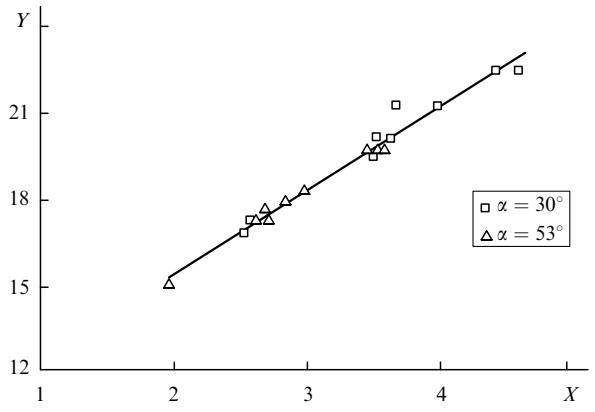

Figure 3. $X - Y$ representation of experimental data on laser thermonuclear fusion in conic targets filled with gaseous deuterium [14, 15, 17, 18].

where ξ is the degree of material compression in the reaction zone. We obtain from here

$$kT = 22.42\varepsilon/m_{\mathrm{D}}, \quad \mu^{4/3}\delta\xi^{2/3} = 1.53 \times 10^{-6}.$$

The values of deuterium plasma temperature T in conic targets, determined using the proposed technique, are given in Table 2 for each experiment.

From the above expressions, we can also estimate the ratio $\mu/\varkappa$, where $\varkappa$ is the coefficient of absorbed laser energy transformation to the thermal energy of thermonuclear plasma. Indeed, $\varkappa = mkT/\varepsilon = \mu m_{\mathrm{D}}\beta\varepsilon/(m_{\mathrm{D}}\varepsilon) = \mu B^{-3}$, hence $\mu/\varkappa = 7.0 \times 10^{-3}B^3 = 0.156$. Since $\varkappa < 1$, $\mu < 0.15$. However, because the estimated transformation coefficient $\varkappa$ does not exceed 0.1, only a small part of deuterium, which is certainly not greater than a few percent of its total mass, is heated to the thermonuclear temperature.

Therefore, in some cases a statistical analysis compensates for the lack of measurable quantities and, moreover, determines the functional dependence of the unmeasured quantities on the parameters of the experiment. The results of statistical analysis for other variables X and Y in the case of spherical targets and a deuterium–tritium plasma are presented in Refs [17, 18]. In particular, the authors of these papers obtained the relation $kT = 9.63\varepsilon/M$ (in units of J ng^{-1}), where M is the total mass of a spherical target and $\mu\delta = 3.05 \times 10^{-3}$.

The conclusions made by applying the statistical approach to experiments with conic targets are in satisfactory agreement with the results of numerical simulation [19, 20] of thermonuclear neutron generation, in which the data of one of experimental diagrams of target shell motion [curve (*2*) in Fig. 2b] were used as the boundary condition. The formulation of the problem took into account the experimentally measured time dependence of the compressing-shell velocity, the target deformation and the ion and electron thermal conduction of the two-temperature deuterium plasma as the temperature limitation mechanism in the collapse of shock waves.

The results presented below were borrowed from Ref. [20], in which the precision of two-dimensional calculations was significantly improved compared to Ref. [19] due to explicit separation of the leading shock wave (in the form of a grid line) during all the time until the wave approaches closely enough the cone apex. Figure 4 shows the time dependences of the spatially maximal ion temperature and the neutron yield. The narrow peaks in the temperature profile correspond to the instants of collapse of the shock wave: the first peak to the collapse of the leading shock wave and the second peak to the collapse of the secondary wave reflected from the shell. One can see that the increase in neutron yield occurs only at these instants, the main contribution to the neutron yield being made by the secondary wave collapse. The stage of adiabatic high-temperature plasma compression is absent due to a small shell mass. The calculated total neutral yield $N = 1.7 \times 10^4$ is in satisfactory agreement with the experimental value of 2.8×10^4. The solution of a spherically symmetric one-dimensional problem, which neglects the target deformation, overestimates the peak values of the ion temperature and, as a consequence, overestimates the neutron yield (approximately 2×10^5). Similar conclusions followed from the results of Ref. [21], where the problem of a shock wave entering a rounded apex of a conic deuterium-filled target was considered by neglecting its deformation.

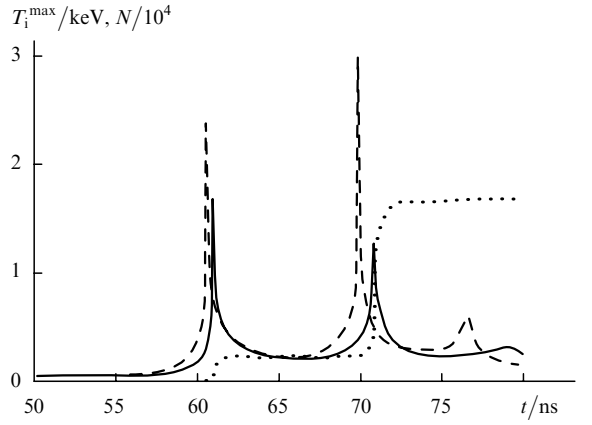

Figure 4. Time dependences of the maximum ion temperature $T_{\mathrm{i}}^{\max}$ calculated by using two-dimensional (solid line) and one-dimensional (dashed line) models and the time dependence of the neutron yield calculated by using the two-dimensional model (dotted line) [20].

Therefore, the neutron yield in the experiments discussed above can be probably explained by an abrupt increase in the ion temperature in a small vicinity of the point of the shock wave collapse. In this case, the inevitable deformation of the walls of the conic target at its apex reduces its neutron yield and thereby plays a stabilising part in a certain sense, which results in close values of the neutron yield despite the significant difference in the initial conditions of the experiments performed (Table 2).

4. Physical processes in conic targets

We review the main theoretical papers that are to a certain extent related to the study of physical processes in conic targets. The review does not pretend to be comprehensive, because these works are rather fragmentary and belong to different realms of physics, in particular, like plasma physics and mechanics of continua. In addition, both analytic and various numerical simulation methods have been used in these studies.

Theoretical estimates and self-similar solutions for the plasma compression scheme in the conic geometry upon the

high-velocity interaction of plungers or targets are presented in [1]. The self-similar solutions apply, in particular, to the compression and heating of material in plane, cylindrical, and spherical cavities. The latter takes place at the cone 'tip'. An estimate of the effect of target walls on the neutron yield upon laser irradiation of conic targets was made on the basis of a simple analytic model in Refs [22, 23]. The problem of spontaneous magnetic field generation upon compression of a laser plasma was analytically considered in Ref. [24] for spherical and conic geometries. The possibilities to experimentally observe the magnetic field in the laser plasma being compressed were discussed.

The most important is the use of numerical simulation techniques, which most completely take into account all the processes in conic targets and serve as an efficient method of investigation, which enables obtaining interesting and physically significant results in many instances.

The numerical simulations of the interaction between plungers and conic targets were performed both in one- and two-dimensional geometries. In the former case, the cone is replaced with a spherical segment, i.e., the cavity-forming material itself is not considered. The problem is thereby reduced to the simulation of spherical shell motion towards the centre. The corresponding calculations, which were carried out in connection with the simulation of spherical laser fusion targets, are rather numerous. The relevant references can be found in reviews [25–30]. However, as regards conic targets, the question arises of whether the real problem can be reduced to the spherical target problem. This is explained by the fact that there exist fundamentally two-dimensional processes of the interaction between the mobile shell and the conic target walls as well as the wall deformation at the final interaction stage. For example, in some cases, high-velocity jets of the material are formed upon the interaction of a plunger with an inclined target wall [31–37]. The development of instabilities in such a flow may, in particular, be responsible for a substantial discrepancy between the experimental neutron yields obtained under similar experimental conditions. In this case, the discrepancy may amount to several orders of magnitude, which was pointed out already in the experimental work [6].

Another evidence for the significance of including the two-dimensionality of processes under study can be found, in particular, in Ref. [9], where the inclusion of two-dimensional effects resulted in a lowering of predicted neutron yield by nearly a factor of 200 compared to the one-dimensional problem. It is therefore reasonable to consider two-dimensional problems. However, at present the number of computational works in this direction is far smaller than the number of works where one-dimensional calculations were performed, which is due to a certain complication of the problem in the two-dimensional case [9, 21, 38–41].

The first works on numerical simulation of the interaction between plungers and a conic cavity [42] were related to the experiment [10] on the explosive initiation of the D–D reaction with the aid of aluminium plungers. These works demonstrated the formation, under certain conditions, of high-velocity cumulative jets inside the targets (Fig. 5). The adequacy of numerical simulations was confirmed by experimental measurements [43]. In these experiments, the average velocity of the material ejected from the opening at the apex of a 30-degree conic target 1.15 mm in diameter was measured in vacuum. For an initial velocity of the 2-mm thick aluminium plunger of 5.4 km s^{-1}, the material velocity

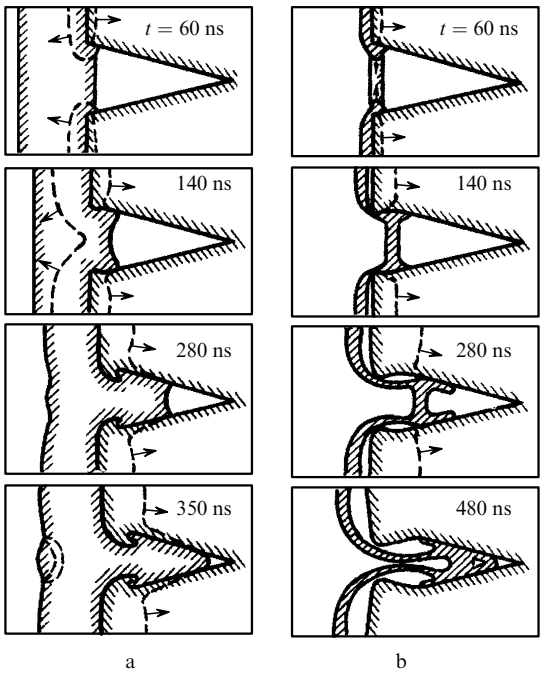

Figure 5. Cumulative effects in the high-velocity interaction of an aluminium plunger with a conic cavity in lead [42, 43]. Use was made of 2-mm thick plungers with a velocity of 5.4 km s^{-1} (a) and of 0.25-mm thick plungers with a velocity of 10 km s^{-1} (b). The time t is counted from the moment the plunger flies up to the target. The dashed lines indicate the positions of shock fronts and the arrows show the direction of their motion.

at a distance of 20 mm from the target edge was equal to 16.5 ± 1.0 km s^{-1}. A numerical solution of this problem yielded a velocity of 17.5 km s^{-1}.

In a more general formulation of the problem, which takes into account the presence of deuterium in the target, this problem was considered in a series of papers summarised in Ref. [44]. In the simulations, wide-range semiempirical equations of metal state [45] and the equation of state of ideal gas (deuterium) were used. The neutron yield was calculated by integrating with respect to time and over the entire volume of deuterium employing the well-known formula for the D–D reaction rate. The plunger and target parameters corresponded to the experiment of Ref. [10]: a 2-mm thick aluminium plunger with a velocity of 5.4 km s^{-1} and a lead target with $\alpha = 53^\circ$ closed with an aluminium lid 0.3 mm in thickness were used. It was shown that in the experiment an annular aluminium jet appeared which was similar to the jet in Fig. 5b in the case of a thin plunger and $\alpha = 28^\circ$. There is no cumulative jet in Fig. 5a, which corresponds to the case of a thick plunger and the same α value. However, for $\alpha = 53^\circ$, this jet appears in the case of a thick plunger as well. By collapsing on the symmetry axis, the annular cumulative jet divides the deuterium volume into two parts and generates high-velocity deuterium jets, which propagate along the symmetry axis, inside the relatively calm deuterium. Despite the occurrence of these jets, the calculated neutron yield turned out to be low. The attempts to explain the emergence of neutrons in the experiment on the basis of viscous heating of the high-velocity deuterium plasma jet in a narrow boundary layer bordering on aluminium [46] also did not meet with success. Therefore, the mechanism of neutron generation in this experiment still remains largely unknown.

Several subsequent theoretical papers were concerned with annular cumulative jets. First we discuss investigations [47, 48] concerning the stability of the jet to axially symmetric perturbations of the inner boundary of the target lid. The initial boundary perturbation was sinusoidal, with an amplitude of 0.2 % of the cone height. The perturbation development is shown in Fig. 6. One can see that the development of the cumulative jet takes place against the background of developed Richtmeyer – Meshkov instability of the major part of the inner lid boundary ($t = 100$ and 160 ns). The 'trace' of this instability persists in the form of low-amplitude nonmonotonies at the jet boundary, which decrease with time. By the instant of jet collapse ($t = 210$ ns) these nonmonotonies vanish and the jet boundary proves to be smooth. Although numerical simulations cannot provide a rigorous answer to the question of whether the flow is stable to perturbations of arbitrary frequency, the calculations performed allow, with a high degree of certainty, a conclusion that the cumulative jets produced in the experiment of Ref. [10] were stable to axially symmetric perturbations of the inner boundary of the target lid.

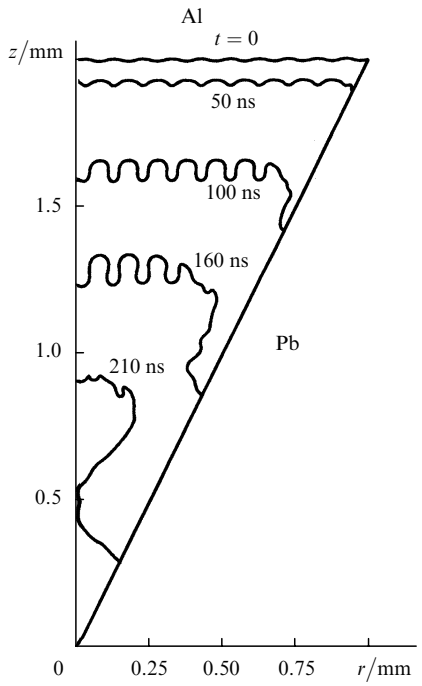

Figure 6. Internal boundary of the aluminium target lid with a sinusoidal initial perturbation in cylindrical coordinates and at sequential points in time [47, 48].

The spontaneous electromagnetic field in the deuterium plasma and the conditions for its penetration into the target were calculated in Ref. [49]. The electromagnetic field problem was formulated similarly to how this is commonly done in laser-plasma simulations (see, for instance, Ref. [50]). The time dependences of the modulus of current density vector at two points inside the target, which are located rather far from the cone, are given in Fig. 7 for two values of α. The axial coordinate of both points is approximately equal to the initial coordinate of the cone apex and the distance to the symmetry axis is equal to ~ 0.5 mm for one point and 1 mm for the other. One can see that for $\alpha = 53^\circ$, when an annular aluminium jet appears, the current density at the former point at first achieves its maximum $\sim 10^{-1}$ A mm^{-2} and then decreases to $\sim 10^{-3}$ A mm^{-2}. The current density at the second point increases to about this value as well. Therefore, the entire above-specified part of the target proves to be covered by Foucault currents with a density of $\sim 10^{-3}$ A mm^{-2}. For $\alpha = 30^\circ$, when the annular cumulative aluminium jet does not appear, the Foucault currents are approximately 10 times weaker, as seen from Fig. 7. The experimental measurement of the Foucault currents in the target can be used to observe the collapse of the annular cumulative jet.

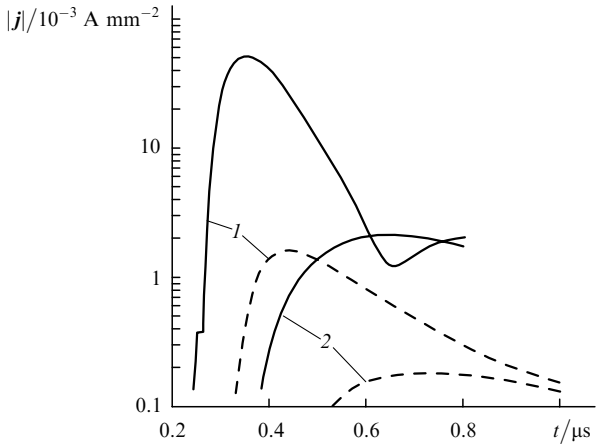

Figure 7. Penetration of spontaneous electromagnetic field into a lead target [49]: time dependences of the modulus of current density vector $\boldsymbol{j}$ for $\alpha = 53^\circ$ (solid curves) and 30° (dashed curves) at a distance of 0.5 (*1*) and 1 mm (*2*) from the symmetry axis.

Let us also mention theoretical paper [51] where the deuterium – tritium fuel compression and thermonuclear energy release in conic targets with additional laser heating were calculated and was also shown that by irradiating these targets by 300 – 400-kJ pulses from a KrF laser, the neutron yield up to 10^{16} neutrons per pulse can be obtained.

The results of simulations of the explosion experiment performed as a continuation of the experiment [10] with an improved launching system are presented in Refs [48, 52]. The presence of deuterium and the cone deformation were not taken into account in these works. The problem of throwing a 30-μm thick aluminium foil with a velocity of 18 km s^{-1} into an empty rigid cone was considered. One of the experimental results presented in review [15] was a decrease in the neutron yield with increasing α from 30° to 60°. Simulations showed that this changes the phase composition of the annular cumulative jet. For $\alpha = 30^\circ$, the jet remains solid, while for $\alpha = 60^\circ$ it consists primarily of a liquid – gas mixture. This suggests that the neutron yield decreases at $\alpha = 60^\circ$ due to cavitation-induced jet destruction.

5. On some possible applications of conic targets

The last decade is characterised by the quickening of interest in different aspects of research related to conic targets and different possibilities of their application. In particular, the possibilities for the application of conic targets in inertial fusion problems were considered in Ref. [53]. Paper [54] contains theoretical estimates of the

use of direct ignition schemes involving cylindrical inertial fusion targets which can have, in particular, conic openings. Paper [55] presents theoretical estimates and results of two-dimensional numerical calculations of conic targets for the ignition of a deuterium–tritium mixture preliminarily compressed by ablation pressure. The heating of compressed fuel by a microexplosion, which takes place in the cone pressurised by this fuel, was proposed in papers [56, 57]. The possibility of cumulative jet production by using cones for compressed fuel heating was studied. The possibility of initiating the thermonuclear reaction in a conic target irradiated by a KrF laser was considered in paper [58]. In an experimental work [59], a conic cavity in gold was employed for the preliminary compression and heating of the shell material, which contained deuterated polyethylene accelerated by a laser pulse. Upon subsequent irradiation of the shell by a short high-power laser pulse through a small opening in the apex of the conic cavity, a neutron yield of 2×10^4 neutrons per pulse was recorded. Some ideas elaborated in approaches of this kind can be traced to an earlier paper [60]. The possibility of producing high-velocity cumulative jets employing laser compression of conic shells and the possibility of employing these jets for the ignition of thermonuclear fuel targets were studied in [61]. The use of conic targets for the explosive graphite-to-diamond transformation was proposed in Ref. [62]. The results of simulations with the inclusion of the equations of graphite-to-diamond transformation kinetics were presented in Ref. [63]. The inclusion of the initial graphite porosity resulted in the discovery of an unexpected property of converging shock waves in porous media [64]. It manifested itself, in particular, in that lowering the initial graphite density in the conic target from the crystalline density (of about 2.26 g cm^{-3}) to 1.7 g cm^{-3} resulted in a three-fold increase in the maximum pressure in graphite.

6. Conclusions

Conic targets are a complicated object for experimental investigation. Their diagnostics has been largely hindered, because all thermonuclear plasma heating processes occur inside a cavity confined in a high-density material. Nevertheless, at present it is possible to advance significantly in this direction. State-of-the-art computational techniques of mathematical physics and significant progress in their computer realisation permit performing numerical simulations of the physical processes in conic targets over a wide range of initial conditions, thereby allowing a more successful planning of the corresponding experiments to realise the desired thermonuclear plasma characteristics. Note that conic targets are of interest not only in connection with the problem of controlled thermonuclear fusion. We believe that their employment in experiments with highly concentrated energy fluxes may open up new possibilities for studying the physical properties of materials at extremely high temperatures, pressures, and densities.

Acknowledgements. The authors thank staff members of the General Physics Institute, the Institute of Chemical Physics Problems, the High Energy Density Research Centre of the Joint Institute for High Temperatures, and the Computing Centre of the Russian Academy of Sciences who were participants and co-authors of Refs [7, 8, 10, 14, 15, 17–20, 42, 43, 52, 62–64]. The authors also thank S.Yu. Gus'kov for stimulating the preparation of this review. This work was supported by the Russian Foundation for Basic Research (Grant Nos 03-02-16627 and 04-01-00051).

References

1. Winterberg F. *Plasma Phys.*, **10** (1), 55 (1968).
2. Bogolyubskii S.L., Gerasimov B.P., Liksonov V.I., Popov Yu.P., Rudakov L.I., Samarskii A.A., Smirnov V.P., Urutskoev L.I. *Pis'ma Zh. Eksp. Teor. Fiz.*, **24** (4), 206 (1976) [*JETP Lett.*, **24** (4), 182 (1976)].
3. Derentowicz H., Kaliski S., Wolski J., Ziolkowski Z. *Bull. L'Acad. Polon. Sci. Ser. Sci. Techn.*, **25** (10), 135 [897] (1977).
4. Derentowicz H., Kaliski S., Ziolkowski Z. *J. Techn. Phys.*, **18** (4), 465 (1977).
5. Derentowicz H. *Zh. Prikl. Mekh. Tekh. Fiz.*, (1), 23 (1989) [*J. Appl. Mech. Techn. Phys.*, **30** (1), 21 (1989)].
6. Derentowicz H., Fruczek M., Kaliski S., et al. *Proc. VII Int. AIRAPT Conf.* (Le Creusot, France, 1979; New York: Pergamon Press, 1980) Vol. 2, p. 1003.
7. Vovchenko V.I., Goncharov A.S., Kas'yanov Yu.S., et al. *Pis'ma Zh. Eksp. Teor. Fiz.*, **26** (9), 628 (1977) [*JETP Lett.*, **26** (9), 476 (1977)].
8. Anisimov S.I., Vovchenko V.I., Goncharov A.S., et al. *Pis'ma Zh. Tekh. Fiz.*, **4** (7), 388 (1978).
9. Mason R.J., Fries R.J., Farnum E.H. *Appl. Phys. Lett.*, **34** (1), 14 (1979).
10. Anisimov S.I., Bespalov V.R., Vovchenko V.I., et al. *Pis'ma Zh. Eksp. Teor. Fiz.*, **31** (1), 67 (1980) [*JETP Lett.*, **31** (1), 61 (1980)].
11. Glass I.I., Sagie D. *Explosive-Driven Hemispherical Implosions for Generating Fusion Plasmas. UTIAS Technical Note No. 233* (University of Toronto, Institute for Aerospace Studies, 1982).
12. Glass I.I., Sagie D. *Phys. Fluids*, **25** (2), 269 (1982).
13. Shyam A., Srinivasan M. *Atomkernenergie. Kerntechnik*, **44** (3), 196 (1984).
14. Vovchenko V.I., Volyak T.B., Kas'yanov Yu.S., Krasyuk I.K., Pashinin P.P., Prokhorov A.M., Semenov A.Yu. Preprint No. 179 (Moscow: General Physics Institute, USSR Academy of Sciences, 1987).
15. Vovchenko V.I., Krasyuk I.K., Pashinin P.P., Prokhorov A.M., Semenov A.Yu., Fortov V.E. *Tr. Inst. Obshchei Fiz. Ross. Akad. Nauk*, **36**, 5 (1992).
16. Vovchenko V.I., Krasyuk I.K., Semenov A.Yu. *Tr. Inst. Obshch. Fiz. Ross. Akad. Nauk*, **36**, 129 (1992).
17. Krasyuk I.K., Pashinin P.P., Semenov A.Yu. *Dokl. Ross. Akad. Nauk*, **336** (1), 43 (1994) [*J. Russian Acad. Sci. Physics–Doklady*, **39** (5), 330 (1994)].
18. Krasyuk I.K., Pashinin P.P., Semenov A.Yu. *Laser Phys.*, **4** (3), 532 (1994).
19. Krasyuk I.K., Pashinin P.P., Semenov A.Yu., Charakhch'yan A.A. *Dokl. Ross. Akad. Nauk*, **354** (3), 324 (1997) [*J. Russian Acad. Sci. Physics–Doklady*, **42** (5), 241 (1997)].
20. Charakhch'yan A.A., Krasyuk I.K., Pashinin P.P., Semenov A.Yu. *Laser Part. Beams*, **17** (4), 749 (1999).
21. Marchenko A.I., Urban V.V. *Tr. Inst. Obshch. Fiz. Ross. Akad. Nauk*, **36**, 112 (1992).
22. Borovskii A.V., Korobkin V.V. Preprint No. 175 (Moscow: General Physics Institute, USSR Academy of Sciences, 1979).
23. Borovskii A.V., Korobkin V.V. *Kvantovaya Elektron.*, **8** (1), 5 (1981) [*Sov. J. Quantum Electron.*, **11** (1), 1 (1981)].
24. Gamalii E.G., Lebo I.G., Rozanov V.B. Preprint No. 97 (Moscow: P.N. Lebedev Physics Institute, USSR Academy of Sciences, 1981).
25. Brueckner K.A., Jorna S. *Revs. Mod. Phys.*, **46** (2), 325 (1974); *Upravlyaemyi lazernyi sintez* (Controlled Laser Fusion) (Moscow: Atomizdat, 1977).
26. Anisimov S.I., Pashinin P.P., Prokhorov A.M. *Usp. Fiz. Nauk*, **119** (3), 401 (1976).
27. Duderstadt J.J., Moses G.A. *Inertial Confinement Fusion* (New York: Wiley, 1982).

28. Kadomtsev B.B. (Ed.) *Lazery i termoyadernaya problema* (Lasers and the Thermonuclear Problem) (Moscow: Atomizdat, 1973).
29. Filyukov A.A. (Ed.) *Problemy lazernogo termoyadernogo sinteza* (Problems of Laser Thermonuclear Fusion) (Moscow: Atomizdat, 1976).
30. Koval'skii N.G. *Lazernyi termoyadernyi sintez* (Laser Thermonuclear Fusion) (Itogi Nauki i Tekhniki. Ser. Fiz. Plazmy. Moscow: VINITI, 1980) Vol. 1, Part 1, p. 166.
31. Walsh J.M., Shreffler R.G., Willing F.J. *J. Appl. Phys.*, **24** (3), 349 (1953).
32. Setchel R.E., Storm E., Sturtervant B. *J. Fluid Mech.*, **56** (3), 505 (1972).
33. Kuz'min G.E., Yakovlev I.V. *Fiz. Goren. Vzryv.*, **9** (5), 746 (1973).
34. Chou P.C., Carleone J., Karpp R.R. *J. Appl. Phys.*, **47** (7), 2975 (1976).
35. Kinelovskii S.A., Trishin Yu.A. *Fiz. Goren. Vzryv.*, **16** (5), 26 (1980).
36. Ternovoi V.Ya. *Zh. Prikl. Mekh. Tekh. Fiz.*, (5), 68 (1984) [*J. Appl. Mech. Techn. Phys.*, **25** (5), 715 (1984)].
37. Zababakhin E.I., Zababakhin I.E. *Yavleniya neogranichennoi kumulyatsii* (Unbounded Cumulation Effects) (Moscow: Nauka, 1988).
38. Mason R.J., Brockway D.V., Lindman E.L. *Dig. VIII Annu. Meet. Division Plasma Physics Amer. Phys. Soc.* (San Francisco, 1976) Report LA-UR-76-2319.
39. Taran M.D., Tishkin V.F., Favorskii A.P., et al. Preprint No. 127 (Moscow: M.V. Keldysh Institute of Applied Mathematics, USSR Academy of Sciences, 1981).
40. Rasskazova V.V., Rogachev V.G., Svidinskaya N.F. *Vopr. Atom. Nauki i Tekhn. Ser. Metod. Program. Chislenn. Reshen. Zadach Matemat. Fiz.*, (3), 39 (1985).
41. Demchenko N.N., Kholodov A.S. *Zh. Prikl. Mekh. Tekh. Fiz.*, (6), 131 (1985) [*J. Appl. Mech. Techn. Phys.*, **26** (6), 877 (1985)].
42. Bushman A.V., Krasyuk I.K., Kryukov B.P., et al. Preprint No. 6-278 (Moscow: Institute for High Temperatures, USSR Academy of Sciences, 1989).
43. Bushman A.V., Krasyuk I.K., Kryukov B.P., et al. *Pis'ma Zh. Tekh. Fiz.*, **14** (19), 1765 (1988) [*Sov. Tech. Fiz. Lett.*, **14** (10), 766 (1988)].
44. Charakhch'yan A.A. *Zh. Prikl. Mekh. Tekh. Fiz.*, **35** (4), 22 (1994) [*J. Appl. Mech. Techn. Phys.*, **35** (4), 506 (1994)].
45. Bushman A.V., Fortov V.E., Kanel G.I., Ni A.L. *Intense Dynamic Loading of Condensed Matter* (Washington: Taylor & Francis, 1993).
46. Charakhch'yan A.A. *Zh. Vych. Matem. Matem. Fiz.*, **33** (5), 766 (1993).
47. Charakhch'yan A.A. *Zh. Prikl. Mekh. Tekh. Fiz.*, **38** (3), 10 (1997) [*J. Appl. Mech. Techn. Phys.*, **38** (3), 337 (1997)].
48. Charakhch'yan A.A. *Plasma Phys. Control. Fusion*, **39** (2), 237 (1997).
49. Charakhch'yan A.A. *Fiz. Plazmy*, **24** (4), 349 (1998) [*Plasma Phys. Reports*, **24** (4), 349 (1998)].
50. Zakharov N.S., Shainoga I.S., Shentsev N.I. *Kvantovaya Elektron.*, **16** (2), 331 (1989) [*Sov. J. Quantum Electron.*, **19** (2), 219 (1989)].
51. Lebo I.G. *Kvantovaya Elektron.*, **30** (5), 409 (2000) [*Quantum Electron.*, **30** (5), 409 (2000)].
52. Lomonosov I.V., Frolova A.A., Charakhch'yan A.A. *Matem. Model.*, **9** (5), 43 (1997).
53. Basov N.G., Lebo I.G., Rozanov V.B., Tishkin V.F., Feoktistov L.P. *Kvantovaya Elektron.*, **25** (4), 327 (1998) [*Quantum Electron.*, **28** (4), 316 (1998)].
54. Gus'kov S.Yu. *Kvantovaya Elektron.*, **31** (10), 885 (2001) [*Quantum Electron.*, **31** (10), 885 (2001)].
55. Caruso A., Strangio C. *Zh. Eksp. Teor. Fiz.*, **124** (5), 1058 (2003).
56. Shmatov M.L. Preprint No. 1759 (St. Petersburg: A.F. Ioffe Physicotechnical Institute, Russian Academy of Sciences, 2002).
57. Shmatov M.L. *Fusion Sci. Technol.*, **43**, 456 (2003).
58. Zvorykin V.D., Lebo I.G., Rozanov V.B. *Bull. Lebedev Phys. Inst.*, (9), 15 (1997).
59. Norreys P.A., Allott R., Clarke R.J., Collier J., Neely D., Rose S.J., Zepf M., Santala M., Bell A.R., Krushelnick K., Dangor A.E., Woolsey N.C., Evans R.G., Habara H., Norimatsu T., Kodama R. *Phys. Plasmas*, **7** (9), 3721 (2000).
60. Winterberg F. *J. Fusion Energy*, **2** (6), 377 (1982).
61. Martinez-Val J.M., Velarde P.M., Piera M., in *Advances in Laser Interaction with Matter and Inertial Fusion* (Singapore: World Scientific Publ., 1997) p. 283.
62. Lomonosov I.V., Fortov V.E., Frolova A.A., Khishchenko K.V., Charakhch'yan A.A., Shurshalov L.V. *Dokl. Ross. Akad. Nauk*, **360** (2), 199 (1998).
63. Lomonosov I.V., Fortov V.E., Frolova A.A., Khishchenko K.V., Charakhch'yan A.A., Shurshalov L.V. *Zh. Tekh. Fiz.*, **73** (6), 66 (2003).
64. Charakhch'yan A.A., Lomonosov I.V., Milyavskii V.V., Fortov V.E., Frolova A.A., Khishchenko K.V., Shurshalov L.V. *Pis'ma Zh. Tekh. Fiz.*, **30** (1), 72 (2004) [*Techn. Phys. Lett.*, **30** (1), 33 (2004)].